CHAPTER VI

EFFECT OF POLY(ETHYLENE OXIDE) AND CATIONIC SURFACTANT COMPLEX STRUCTURE ON TURBULENT FRICTION FACTOR

6.1 Abstract

We study the dependence of friction factor on Reynolds number using a Couette cell containing aqueous solutions consisting of poly(ethylene oxide) (PEO), cationic surfactant, hexadecyltrimethylammonium chloride (HTAC) and their complexes. In our Couette geometry, the onset of turbulent transition occurs at Re ≅ 940. By varying PEO molecular weight and concentration, the minimum friction factor occurs at an optimum concentration, c^*_{PEO}, which scales inversely with PEO molecular weight. For aqueous HTAC solutions, the friction factor decreases with increasing HTAC concentration and levels off at an optimum concentration, c^*_{HTAC}, whose value is comparable to the critical micelle concentration (CMC). The friction factor of aqueous HTAC solutions increases with excessive counter-ions added due to the presence of thread-like micelles. For aqueous PEO-HTAC solutions, an addition of HTAC at maximum binding concentration (MBC) to a non-drag reducing low M_w PEO solution can induce a decrease in friction factor, possibly due to increased hydrodynamic volume and extensional viscosity. Addition of counter-ion to PEO-HTAC complex decreases the friction factor because of the stabilized PEO-HTAC complex formation, and possibly due to the reduction in the PEO chain rigidity. Pure polymer solutions at c^*_{PEO} generally exhibit the lowest friction factor values when compared with those of pure HTAC and PEO-HTAC complex solutions.

6.2 Introduction

Turbulent drag reduction, DR, is a flow phenomenon in which small amounts of certain additives, e.g. high molecular weight polymers, surfactants or solid particles can dramatically reduce the skin frictional resistance of a solid surface and a fluid in turbulent flow [1-3]. This phenomenon has also been known as "Toms

effect" since it was originally discovered by Toms [4]. He observed a reduction of friction factor for dilute solution of poly(methyl methacrylate) in monochlorobenzene in turbulent pipe flow. It is now well known that turbulent drag reduction depends on many factors including polymer molecular weight, polymer type, concentration, temperature and solvent type [5-9]. Numerous applications of DR can be found in the transport of crude oil and shipping industries, in fire fighting equipment, in drainage and irrigation systems, in hydro-power systems, and in improvement of blood flow in partially blocked arteries in biomedical studies [10-14].

Although DR was discovered more than fifty years ago, DR mechanisms by drag reducing additives are not completely understood and a number of chemical, mechanical and hydrodynamic aspects remain to be studied. The early mechanism for drag reducing polymers was given by Virk [15] who proposed that at the onset of turbulent drag reduction the duration of a turbulent burst is of the order of the terminal relaxation time of a macromolecule, and concluded that energy dissipation via macromolecular extension is involved in the mechanism of drag reduction. Hlavacek et al. [16] proposed that, in turbulent flow, the solvent contains microdisturbances or turbulence precursors. A macromolecule can suppress turbulence by pervading two or more of these microdomains simultaneously and hindering their free movement and growth. Lumley [17-19] suggested that there is a critical value of wall shear stress, at which macromolecules become expanded due to the fluctuating strain rate. He pointed out that in the laminar sublayer close to the wall, polymer coils are not greatly deformed and viscosity does not increase greatly above that of the solvent alone. In the turbulent zone, the macromolecular expansion yields a dramatic increase in viscosity which damps out small dissipative eddies and reduces momentum transport from the buffer layer towards the laminar sublayer, resulting in a thickening of the sublayer and a reduction of the drag. He also emphasized that drag reduction occurs only when the relaxation time of the polymer solution is larger than the characteristic time scale of the turbulent flow. Ryskin [20] developed the yo-yo model which refers to the proposed mechanism in which polymer molecules unravel in an extensional flow field associated with turbulence. The central portion of the chain straightens, while the end portions remain coiled. When the flow becomes weak, the polymer chain retracts into a fully-coiled state.

The taut central portion generates a large stress and facilitates viscous dissipation of turbulent kinetic energy. De Gennes [21,22] developed a model based on the Kolmogorov energy cascade theory, and considering the ability of polymer molecules to store elastic energy upon deformation. When this elastic energy is comparable to the kinetic energy of a particular turbulent eddy, the energy cascade is suppressed.

High molecular weight polymers and surfactants have received considerable attentions among available drag reducing additives [23,24]. Extensive studies have been carried out for the drag reducing polymers; however, polymers are more susceptible to high mechanical and thermal degradation compared to surfactants. The degradation of polymers reduces their drag reducing effectiveness and makes them unsuitable for circulation systems. Certain surfactants form large wormlike or network microstructures in solution which are thermodynamically stable and self-assemble quickly after degradation and restoring drag reducing power. For this reason, they have become of increasing interest as drag reducing additives in the last decade [25-27].

Many drag reduction experiments have been carried out by using pipe flow apparatus [1,9] since it provide a realistic and quantitative testing of polymer drag reduction. However, this experimental system is voluminous and the measurements consume both time and sample solution. In a recent study, turbulent drag reduction measurements were carried out by using a Couette cell [28,29]. The apparatus generates a turbulent flow under a nonuniform mean velocity field with well controlled conditions In our work, the effects of polymer concentration, polymer molecular weight, surfactant concentration, type of drag reducing additives and ionic strength on turbulent drag reduction and friction factor were investigated. In particular, the effect of the polymer-surfactant complex structure will be reported.

6.3 Experimental Section

Poly (ethylene oxide) (PEO) of various quoted molecular weights $1.00x10^5$, $3.00x10^5$, $6.00x10^5$, $9.00x10^5$ and $40.0x10^5$ g/mol, designated as PEO1, PEO3, PEO6, PEO9 and PEO20 were purchased from Aldrich Chemical Co. and used

without further purification. The cationic surfactant was Hexadecyltrimethylammonium Choride, (HTAC, $C_{16}H_{33}N(CH_3)_3Cl$), a commercial product donated by Unilever Holding Inc., was used as received. The surfactant solution contains 50 %HTAC, 36 % H_2O and 14 % isopropanol. Analytical grade sodium chloride (NaCl), at 99.5 % minimum assay (Carlo Erba Reagenti Co.) was used to vary ionic strength of the complex solutions. Distilled water was used as our solvent after two times filtration through 0.22 μm Millipore membrane filters to remove dust particles. PEO stock solutions of 0.5 %(w/v) were prepared and stirred gently at room temperature for 4 to 30 days, depending on polymer molecular weight. The polymer-surfactant complex solutions were prepared as %w/v in distilled water at room temperature by dissolving PEO stock solutions in distilled water and by gentle stirring for 24 h at room temperature. Surfactant and polymer-surfactant complex solutions were prepared by adding appropriate amounts of HTAC and NaCl into mixtures of distilled water and polymer stock solutions and by gentle stirring for 24 h at room temperature. For light scattering measurements, the polymer-surfactant complex solutions were centrifuged at 10,000 rpm for 15 min and then filtered through 0.45 μm Millipore membranes. All measurements were carried out at the temperature of 30°C.

6.4 Results and Discussion

6.4.1 Characterization of PEO in aqueous solution

Table 6.1 shows physical parameters obtained from static and dynamic light scattering measurements of aqueous PEO solutions of various molecular weights at 30°C. The average weight molecular weight, M_w, obtained from static light scattering measurements of PEO1, PEO3, PEO6, PEO9 and PEO20 are $0.91x10^5$, $3.04x10^5$, $6.06x10^5$, $8.03x10^5$ and $17.90x10^5$ g/mol, respectively. The diffusion coefficient, D_o and hydrodynamic radii, R_h obtained from the dynamic light scattering measurements vary with PEO molecular weight as expected. The diffusion coefficient, D_o decreases from $13.3x10^{-12}$ m^2/sec for PEO1 to $3.2x10^{-12}$ m^2/sec for PEO20. The corresponding R_h increases from 16.69 nm for PEO1 to 70.24 nm for

PEO20. The normalized second cumulant, $\mu_2/\overline{\Gamma}^2$ is a measure of the variance of the size distribution. Here, we find that $\mu_2/\overline{\Gamma}^2$ systematically decreases from 0.50 to 0.32 with increasing molecular weight. These results indicate that our PEO samples are highly polydisperse and the polydispersity is higher for the lower molecular weight samples. A correlation between D_o and M_w ($D_o = kM_w^a$) can be found in which the scaling exponent 'a' and the prefactor k are 0.50 and 3.82×10^{-9} m^2/sec, respectively. It is noted that the variation of 'a' should satisfy a ~ 0.60 for flexible polymer chains in good solvents [33,34]. Thus, the small value of 'a' is probably a consequence of the fact that the lower molecular weight PEO samples have higher polydispersity.

6.4.2 Characterization of HTAC, PEO-HTAC and PEO-HTAC-NaCl complexes in aqueous solution

Table 6.2 tabulates the physical parameters obtained from dynamic light scattering measurement of aqueous HTAC, PEO-HTAC and PEO-HTAC-NaCl complexes solutions at 30°C. Uncertainties indicate standard deviations obtained from repeated measurements of the same samples. The dynamic light scattering parameters determined are the diffusion coefficient, D_o, the hydrodynamic radius, R_h, and the normalized second cumulant, $\mu_2/\overline{\Gamma}^2$, of solutions in the limit of very dilute condition. Initially, the parameters listed above were measured at high HTAC concentrations and then they were extrapolated to particular HTAC concentrations of interest. For aqueous HTAC and NaCl-HTAC solutions, D_o, R_h and $\mu_2/\overline{\Gamma}^2$, listed in Table 5.2 were determined at the critical micelle concentration, CMC of these solutions. The values of CMC are 1.3, 0.7 and 0.6 mM for the HTAC, HTAC + [NaCl]/[HTAC] = 1/1 and HTAC + [NaCl]/[HTAC] = 5/1 in aqueous solutions. However, for aqueous PEO-HTAC and PEO-NaCl-HTAC solutions, the parameters, D_o, R_h, and $\mu_2/\overline{\Gamma}^2$ were determined at the HTAC concentration of 5.0 mM, the maximum HTAC concentration used in friction factor measurements. At this HTAC concentration, surfactant micelles are bound to polymer chains. In pure HTAC

solution, the diffusion coefficient, D_o is at $170x10^{-12}$ m^2/s but decreases from 99.8 to $90.7x10^{-12}$ m^2/s with increasing mole ratio of NaCl to HTAC from 1 to 5, respectively. The hydrodynamic radius, R_h of pure HTAC solution is 1.31 nm and increases from 2.23 to 2.45 nm with increasing mole ratios of NaCl to HTAC from 1 to 5, respectively. On the contrary, for the aqueous PEO-HTAC solution, PEO6_40+HTAC, the D_o is at $3.98x10^{-12}$ m^2/s and decreases slightly from 4.92 to $4.59x10^{-12}$ m^2/s for PEO6_40+[NaCl]/[HTAC] = 1/1 and PEO6_40+[NaCl]/[HTAC] = 5/1, respectively. The values of R_h found in aqueous PEO6_40+HTAC, PEO6_40+[NaCl]/[HTAC] = 1/1 and PEO6_40+[NaCl]/[HTAC] = 5/1 are 55.9, 45.1 and 48.4 nm, respectively. The data from high molecular weight PEO, PEO20, are also consistent with that of low molecular weight PEO, PEO6. D_o varies from 2.40, 3.08 and $2.90x10^{-12}$ m^2/s and the corresponding R_h varies from 92.7, 72.2 and 76.4 for PEO20_15+HTAC, PEO20_15+[NaCl]/[HTAC] = 1/1 and PEO20_15+[NaCl]/[HTAC] = 5/1, respectively. Here, we find that addition of salt to PEO-HTAC solutions first shifts R_h to a lower value, and then R_h increases with further increase in the mole ratio of NaCl to HTAC to five. Our results are consistent with the previous published data reported by Khine et al. [35], who studied an aqueous solution of PEO-HTAC and a ternary PEO-HTAC solution in 0.1 M KNO_3. They reported that an addition of 0.1 M KNO_3 to PEO-HTAC solution can reduce R_h due to the effects of polymer chain contraction via the electrostatic screening and the dissociation of multichain complexes.

Next, we report data of the normalized second cumulant, $\mu_2 / \bar{\Gamma}^2$ which indicates a measure of variation in the micelle or complex size. For the HTAC systems, $\mu_2 / \bar{\Gamma}^2$ varies between 0.16 and 0.07 for the aqueous HTAC and [NaCl]/[HTAC] = 5. For the PEO-HTAC systems, $\mu_2 / \bar{\Gamma}^2$ of PEO6_40+HTAC and PEO6_40+[NaCl]/[HTAC]=5/1 are 0.83 and 0.23, respectively. The data clearly suggest that an addition of salt reduces polydispersity or assists in stabilizing micelle or complex structures formed.

6.4.3 Friction factor vs. Reynolds number

6.4.3.1 Friction factor vs. Reynolds number of water

In our experimental work, all friction factor measurements were carried out using a double Couette cell, DCU, and a single Couette cell, SCU, where temperature was fixed at 30°C. The friction factor, f and Reynolds number, Re, of sample solutions were calculated by equations 11 and 12, respectively. Figure 6.1 illustrates a plot of friction factor, f versus Reynolds number, Re of solvent or water at 30°C. As can be seen from this plot, there is a change in the slope of f vs. Re at Re equal to 1000 (shear rate, $\dot{\gamma} = 68.29\ s^{-1}$). Previous experimental studies have been carried out to investigate flow transitions in Couette geometry. Nakken et al. (2001) [28] measured the friction factor versus Reynolds number of water at 20°C by using a standard double-gap sample holder with the radius ratio, η, and the aspect ratio, α, of 0.98 and 222, respectively. They found that the change in the slope occurs at Re equals to about 40. This transition represents the initial instability or the onset of the Taylor instability. The slope is -1.00 in the region corresponding to laminar flow and -0.60 in the region with the well defined Taylor vortices. Walowit *et al.* (1964) [36] reported that an increase in radius ratio, η, of the Couette geometry would result in a decrease in the critical Re for the Taylor instability. They also found that at the radius ratio η equals to 0.40 (the radius ratio of our Couette geometry), the critical value of Re for Taylor instability can be estimated to occur 68.

For turbulent transition, Coles (1965) [37] Koschmieder (1979) [38], and Fenstermacher *et al.* (1979) [39] reported that at the radius ratio, η equal to 0.88, the transition towards fully turbulent flow in a Couette geometry occurs at Re equals to $23.50Re_{c,T}$ where $Re_{c,T}$ is the critical Reynolds number for the onset of Taylor instability. From the data of Walowit et al. [36], Coles [37], Koschmieder [38], and Fenstermacher [39], we can estimate that the onset of turbulent transition should take place in our cell at $Re \cong 1600$. Hence, we identify the change in the slope of f vs. Re in Figure 1 as the turbulent transition. However, the critical Re of the onset of Taylor instability cannot be observed from figure 1 due to the limitation of the torque

sensor of our fluid rheometer because the minimum Re investigated is about 100. The correlation between friction factor and Reynolds number of Figure 1 follows a power law consisting of two regimes with a scaling exponent of -1.0 in the first regime corresponding to some pre-transition flows, and a scaling exponent of -0.8 in the second regime. Noted that many previous studies investigated drag reduction by using small gap Couette device ($\eta = 0.80 - 0.90$) [37 - 41] since this type of Couette generates the instability of fluid flow at low Re. In narrow gap Couette cell, the flow transition takes place smoothly starting from laminar flow, Taylor vortex flow, wavy Taylor vortex flow, the combination of Turbulent and Taylor flows and fully turbulent flow [37,38,39]. However, our experiment was carried out by using wide gap Couette cell ($\eta = 0.40$). In wide gap Couette cell, we might only have laminar flow, and then small scale fluctuations settled in with laminar boundary layers develop along both walls. We bypass all together Taylor sequences. The first regime observed from the plot of f versus Re would be corresponding to weak turbulence and the flow would becomes a strong turbulence at second regime or at high Re number. In addition, the scaling exponents of the plot of f versus Re in wide gap Couette are lower than those observed in narrow gap. This might occur due to the existence of end effect [42]. The wider gap of Couette, the higher end effect performs. The end effect appears to scale inversely with Reynolds number and might shift the scaling exponents to lower value.

6.4.3.2 Effect of PEO concentration on f vs. Re

Figure 6.2 shows the dependence of friction factor, f, on Reynolds number, Re, for PEO M_w of 6.06×10^5 g/mol (PEO6) at various PEO concentrations, and at 30°C. PEO concentrations investigated are 0, 10, 20, 40, 60, 200, and 300 ppm. As can be seen from this figure, the correlation of f vs. Re decreases as PEO concentration increases from 0 up to 40 ppm. We may identify a PEO concentration as the optimum PEO concentration, c^*_{PEO}, a concentration at which a minimum friction factor is obtained. Beyond c^*_{PEO}, the correlation of f vs. Re increases toward an asymptotic correlation, independent of PEO concentration up to PEO

concentration equal 300 ppm. We can summarize that the optimum PEO concentration, c^*_{PEO} divides the effect of PEO concentration on friction factor into two regimes. At $c < c^*_{PEO}$, the friction factor decreases with PEO concentration. This observation is generally consistent with the viscous theory [17-19] and the elastic [21, 22] theory on drag reduction. From the viscous theory, the expansion of polymer chain by velocity gradient and the relaxation due to the elasticity of polymer molecules occurs simultaneously on the same time scales in a turbulent flow. These behaviors lead to an increase in the hydrodynamic volume, an increase in extensional viscosity, a reduced momentum transport in the buffer layer, and consequently a reduction in the wall shear stress or the friction factor. In the elastic theory, as polymer chains deform, they are capable of storing some of the cascading energy of turbulent eddies of various sizes. Thus the kinetic energy is not fully cascaded down to smaller scales as it normally would, resulting in a larger Kolmogorov microscale which is eventually dissipated, and thus a reduced wall shear stress. At $c > c^*_{PEO}$, increasing polymer concentration does not induce a further decrease in the friction factor. At sufficiently high PEO concentrations, interchain interactions and the total chain volume cause drastic increases in shear and extensional viscosities and hence they can overwhelm the drag reduction effect.

6.4.3.3 Effect of PEO molecular weight on f vs. Re

Figure 6.3 illustrates the dependence of friction factor, f, on Reynolds number, Re, of PEO aqueous solutions of various molecular weights. In this figure, the PEO concentration was fixed at the optimum concentrations, c^*_{PEO}, the PEO concentration for each molecular weight of PEO. From our previous results [43], the values of c^*_{PEO} are 50, 40, 30, and 15 ppm for PEO of M_w equal to 3.04×10^5, 6.06×10^5, 8.03×10^5, and 17.9×10^5 g/mol, respectively. We find that no drag reduction takes place for PEO1 or PEO M_w 0.91×10^5 g/mol. In agreement with previous results [23,29] and our previous work [43], we find that the higher molecular weight PEO possess lower optimum PEO concentrations and there is a critical molecular weight of polymer where drag reduction does not occur. The result from Figure 3 shows that the correlation of f vs. Re of the PEO solutions at their c^*_{PEO} decreases with

increasing PEO molecular weight. This indicates that a higher molecular weight PEO has greater drag reduction effectiveness. This observation is consistent with either the viscous [17-19] or the elastic [21, 22] theories of drag reduction as discussed above. We further note that the optimum hydrodynamic volume fraction is numerically similar for each PEO sample, $c^*_{PEO}[\eta] \sim 0.0145 \pm 0.002$, and two orders of magnitude smaller than the overlap value, $c^*_{PEO}[\eta] \sim 1.0$. The data are consistent with the previous observations by Nakken et al [29] who found that drag reduction by polymer occurs mostly at a hydrodynamic volume fraction of approximately below 0.2.

6.4.3.4 Effect of HTAC on f vs.Re

The effect of surfactant on the correlation of f vs. Re in aqueous solutions of various surfactant concentrations is illustrated in Figure 6.4. HTAC concentration was varied from 0 to 5 mM at 30°C. At low HTAC concentrations (0 – 1.7 mM), the correlation of f vs. Re decreases with increasing concentration up to the optimum concentration, c^*_{HTAC}, which is equal to 1.7 mM where the wall shear stress is minimum. At $c_{HTAC} > c^*_{HTAC}$, the correlation of f vs. Re increases with increasing HTAC concentration toward an asymptotic correlation when HTAC concentration reaches 5 mM. Characterization data of HTAC in an aqueous solution obtained from the previous studies [43] shows that the CMC (a critical micelle concentration of surfactant at which formation of micelles occurs) of HTAC occurs at approximately 1.3 mM. Thus we are apparently seeing a gradual decrease in the friction factor prior to the micelle formation. Our result maybe compared with the previously published data [44-46] where they found that for dilute solutions containing a cationic surfactant and counterions a thread-like micelle structure formed is necessary for the surfactant to be an effective drag reducer. On the other hand, the reduction of friction factor may be related to lowering of the surface tension by free surfactants, or turbulence itself may favor free surfactants to form micelles even at very low surfactant concentration. A recent study by B Lu et al. (2004) [47] reported that the reduction in the wall shear stress is accomplished by the additive-introduced

viscoelastic stress generated by HTAC and sodium salicylate counter-ions. He postulated that surfactant additives may have dual effects on frictional drag: (1) introduce viscoelastic shear stress which increases the frictional drag; and (2) dampen some turbulent vortex structures, or the decrease the turbulent shear stress/momentum transport, and hence the decrease in the friction factor. Since the second effect is greater than the first one, drag reduction results.

6.4.3.5 Effect of counter-ion on f vs. Re

Figure 6.5.1 shows the correlation of f vs. Re for a) pure aqueous solution; b) the aqueous solution with HTAC at 5.0 mM; and c) the aqueous solution with HTAC at 5.0 mM and NaCl added at the mole ratio [NaCl]/[HTAC] equal to 5/1. In this figure, we find the changes in slope of f vs. Re occur at Re equal to 1000, 420 and 900 for the systems of pure water, HTAC 5.0 mM and HTAC 5.0 mM + [NaCl]/[HTAC] = 5/1, respectively. The changes in slope correspond to the transition towards fully turbulent flow. In our systems investigated, we observe a decrease in the correlation of f vs. Re at all Re in the presence of HTAC at 5 mM. This HTAC concentration at 5.0 mM is well above CMC value of HTAC in aqueous solution; CMC_{HTAC} = 1.3 mM. In the presence of added salt, the correlation of f vs. Re increases above that without salt.

Figure 6.5.2 illustrates the schematic drawings of micelle structures of HTAC in aqueous solution with and without NaCl added. For the aqueous solution of HTAC 5.0 mM in salt free solution, most surfactants form spherical micelles; however, there are some free surfactants left in the solution. For the aqueous solution of HTAC 5 mM with salt added, a thread-like micellar network microstructure appears due to the neutralization of the positive charges on the surfactant headgroups by the negative charges of the counterion molecules [44-46]. Our work demonstrate that the friction factor increases with exessive counterions added as a result of the increased viscous resistance because of the presence of thread-like micelles. This should be contrasted with the work of [46] who reported that the friction factor is reduced when salt is added at relatively small counter-ion/surfactant ratios.

6.4.3.6 Effect of HTAC concentrations on f vs. Re: Low molecular weight PEO

The influence of HTAC concentration on drag reduction for aqueous solutions of low molecular weight PEO and HTAC complexes was investigated and shown in Figure 6.6. Figure 6.6.1 shows the dependence of friction factor, f vs. Reynolds number, Re, at various HTAC concentrations at 30°C for the complex solutions of PEO1 (PEO M_w $0.91x10^5$ g/mol at 200 ppm and HTAC which is designated as HTAC/PEO1_200). The data shows that with increasing HTAC concentration from 0 to 2.0 mM, the correlation f vs. Re decrease towards a minimum value at the optimum HTAC concentration, $c^*_{HTAC\text{-}PEO}$, of 1.3 mM. Above this optimum concentration, the correlation f vs. Re increases towards an asymptotic correlation at HTAC concentration equal to 2.0 mM. The HTAC concentration equal to 2.0 mM is very close to the CMC value of HTAC/PEO1_200; i.e., $CMC_{HTAC/PEO1\_200}$ = 1.90 mM. No drag reduction occurs when HTAC concentration is greater than the CMC for this HTAC-PEO complex solution. Previously, we may recall that the wall shear stress does not decrease for the aqueous solution of PEO M_w $0.91x10^5$ g/mol at 200 ppm in the absence of HTAC, as evidenced in our previous work [43]. Thus, an addition of small amounts of HTAC to a non-drag reducing PEO solution can induce turbulent drag reduction. Figures 6.6.2a – 6.6.2d illustrate the schematic drawings of the polymer and polymer-surfactant complexes of PEO1 and HTAC at various concentrations in aqueous solutions. (a) PEO1_200; PEO M_w $0.91x10^5$ g/mol 200 ppm. The linear flexible polymer molecules exist as a random coil in the aqueous solution. (b) PEO1_200 + HTAC 0.8 mM; PEO M_w $0.91x10^5$ g/mol 200 ppm and HTAC concentration equal to 0.8 mM. The cationic surfactants bind to polymer and the polymer chains were expanded due to the repulsive force between positive head group of surfactants. (c) PEO1_200 + HTAC 1.3 mM; PEO M_w $0.91x10^5$ g/mol 200 ppm and HTAC concentration equal to 1.3 mM. Here, we find the minimum value of the friction factor when HTAC concentration is equal to 1.3 mM. This HTAC concentration is slightly smaller than the MBC or the maximum binding concentration of PEO1_200 + HTAC; $MBC_{PEO1\_200+HTAC}$ = 1.80 mM. This MBC is defined as the concentration at which polymer chains are bound and saturated with surfactant molecules. Thus, at this

HTAC concentration, polymer chains are fully expanded due to electrostatic repulsions between bound surfactant molecules [33]. Consequently, the chain hydrodynamic radius, R_h, and the extensional viscosity increase to their maximum values at MBC. (d) PEO1_200 + HTAC 2.0 mM; PEO M_w $0.91x10^5$ g/mol 200 ppm and HTAC concentration equal to 2.0 mM. Above the critical micelle concentration of PEO1_200+HTAC; $CMC_{PEO1\_200+HTAC}$ = 1.90 mM, spherical micelles form in the aqueous solution and also bind onto the polymer chains. In addition, the excess surfactant causes electrostatic screening between bound micelles, and therefore, chain contraction occurs. We may explain the drag reduction behavior of these HTAC-PEO complexes by two mechanisms. First, unassociated HTAC molecules in HTAC/PEO mixtures may act to produce drag reduction by itself, as evidenced by the data of Figure 4. Second, which may coexist with the first, binding of HTAC molecules to PEO chains occurs, resulting in a chain expansion, and an increase in hydrodynamic volume and extensional viscosity. These two mechanisms promote drag reduction in PEO-HTAC complex.

6.4.3.7 Effect of HTAC concentrations on f vs. Re of high molecular weight PEO-HTAC complex solutions

Next, we investigate the effect of HTAC concentration on the correlation of f vs. Re of high molecular weight PEO6 (PEO M_w 6.06x105 g/mol) and HTAC in aqueous solution at 30°C. Figure 6.7.1 illustrates the correlations of friction factor, f, versus Reynolds number, Re, of aqueous solutions of PEO6 at 40 ppm and HTAC at various concentrations. This PEO concentration is the optimum PEO concentration or c^*_{PEO}, the PEO concentration at which f of pure PEO6 solution is minimal. The correlation of friction factor monotonically increases with increasing HTAC concentration from 0 to 2.0 mM. This finding can be contrasted with the results of the low molecular weight PEO1, where we find that adding surfactant initially reduces friction factor. The schematic drawings of PEO6_40 and PEO6_40+HTAC in aqueous solutions are shown in Figures 6.7.2a and 6.7.2b, respectively. (a) PEO6_40; PEO M_w $6.06x10^5$ g/mol at 40 ppm. Polymer chains are fully stretched due to turbulence. (b) PEO6_40+HTAC (PEO M_w $6.06x10^5$ g/mol at 40 and HTAC).

Polymer chains and surfactant molecules combine to form complexes. To explain this behavior, we first note that the increase in the friction factor occurs at very low levels of HTAC; below the nominal CAC ($CAC_{PEO6\_40+HTAC}$ = 0.18 mM). It appears that the CAC of PEO6_40+HTAC solution is reduced by turbulence. More surfactant molecules can bind onto polymer chains which results in the increased rigidity of the polymer-surfactant complexes. Furthermore, when HTAC concentration is greater than MBC of PEO6_40+HTAC solution ($MBC_{PEO6\_40+HTAC}$ = 0.20 mM.) the hydrodynamic volume of PEO-HTAC complex is reduced due to the polymer chain contraction via electrostatic screening effect between bound micelles.

6.4.3.8 Effect of counterion on f vs. Re of PEO-HTAC complex solutions

Figure 6.8 shows the effect of ionic strength on the polymer – surfactant complex and the correlation of f vs. Re. The correlations of f vs. Reynolds number shown in Figure 6.8 are: a) water; b) PEO6_40+HTAC 5.0 mM; c) PEO6_40+HTAC 5.0 mM+[NaCl]/[HTAC] = 1/1 and d) PEO6_40+HTAC 5.0 mM+[NaCl]/[HTAC] = 5/1. Here, PEO6_40 is PEO M_w of $6.06x10^5$ g/mol at 40 ppm. The HTAC concentration was fixed at 5.0 mM and the mole ratio of NaCl to HTAC was varied from 0, 1 and 5, respectively. The correlation of f vs. Re of water and PEO6_40+HTAC 5.0 mM in the salt free solution are nearly the same. We may note that the HTAC concentration is well above MBC. On the other hand, with added salt, the correlation dramatically decreases with increasing mole ratio of [NaCl]/[HTAC]. Figures 6.8.2a – 6.8.2b illustrate the schematic drawings of PEO6_40 + HTAC in salt free aqueous solution and in aqueous solution with salt added, respectively. In the salt free aqueous solution, binding of micelles on the multichain polymer-surfactant complexes occurs in the solution, leading to an increase in hydrodynamic volume of polymer-surfactant complex. Simultaneously, those bound micelles enhance polymer chain rigidity and reduce the overall elasticity. In the presence of salt, the number of bound HTAC molecules per chain increases or the added salt stabilizes the binding of HTAC micelles to the polymer due to the reduction of electrostatic repulsions between surfactant head groups [33]. In addition, the hydrodynamic volume of PEO-

HTAC complex is reduced due to effects of polymer chain contraction via the electrostatic screening and the dissociation of multichain complexes. The decrease in the friction factor upon addition of salt to PEO-HTAC complex is suggested to be related to the stabilized PEO-HTAC complex formation, and possibly due to the decrease in the PEO chain rigidity resulting from the dissociation of multichain complexes.

6.4.3.9 Effect of various types of drag reducing additives in aqueous solutions

The effect of various types of drag reducing additives on friction factor, f versus Reynolds number, Re is summarized and shown in Figure 6.9. This figure shows the dependence of friction factor versus Reynolds number of: a) water, b) PEO6_40, c) HTAC 5.0 mM and d) PEO6_40+HTAC 5.0 mM. Apparently, for the pure polymer solution of PEO6_40 (PEO M_w $6.06x10^5$ g/mol at 40 ppm) it exhibits the lowest correlation of f vs. Re. For the surfactant solution, HTAC at 5.0 mM, the friction factor is lower than that of water but the drag reduction effectiveness is smaller when compared to that of the pure polymer solution. For the polymer-surfactant complex solution of PEO6_40+HTAC 5.0 mM, the correlation is nearly the same as that of pure water. In this case, the concentration of PEO6 is at 40 ppm the optimum PEO concentration, c^*_{PEO}. The HTAC concentration is at 5.0 mM, well above CMC which is 1.3 mM. The small reduction of friction factor of the pure PEO and HTAC solutions can be explained due to an increase in hydrodynamic volume, an increase in extensional viscosity, and possibly the elasticity of polymer and micelle structures. When HTAC is added to PEO, the correlation of f vs. Re increases with HTAC concentration. The finding may be explained in terms of the increased rigidity of the complex and the multichain association.

6.5 Conclusions

The dependence of friction factor on Reynolds number of poly(ethylene oxide) (PEO), cationic surfactant (HTAC) and their complexes in aqueous solutions

was investigated systematically with regards to various variables; polymer concentration, polymer molecular weight, surfactant concentration and ionic strength. Consistent with previous published data, the onset of turbulent transition takes place at Re ≅ 1600. High molecular weight of PEO and PEO concentration up to the optimum PEO concentration, c^*_{PEO} promote the reduction of friction factor. In aqueous HTAC solution, the friction factor decreases with increasing HTAC concentration and levels off at an optimum concentration, c^*_{HTAC}, whose value is comparable to the critical micelle concentration (CMC). Furthermore, the friction factor of aqueous HTAC solutions increases with excessive counter-ions added due to the increased viscosity resulting from the presence of thread-like micelles. For aqueous PEO-HTAC solutions, binding of HTAC to PEO chains induces polymer chain expansion and the magnitude of the hydrodynamic volume of the polymer-surfactant complexes. This behavior results in the minimum of friction factor at maximum binding concentration (MBC). Addition of counter-ion to PEO-HTAC complex decreases the friction factor due to the stabilized PEO-HTAC complex formation, and possibly due to the decrease in the PEO chain rigidity. It appears that pure polymer solution at c^*_{PEO} exhibits the lowest friction factor when compare to pure HTAC and PEO-HTAC complex solutions.

6.6 Acknowledgements

S. Suksamranchit would like to acknowledge the financial support from the Thailand Research Fund (TRF), the RGJ grant no. PHD/0149/2543. This work was partially supported by the fund from MTEC, grant no. MT-43-POL-09-144-G, the fund from the ADB Consortium Grant, and the Conductive and Electroactive Polymers Research Unit, CU. AMJ acknowledges the financial support through NSF, award number DMR 0080114.

6.7 References

1. P. S. Virk and H. Baher, The effect of polymer concentration on drag reduction, *Chemical Engineering Science*, 25 (1970) 1183.
2. G.D. Rose and K.L. Foster, Drag reduction and rheological properties of cationic viscoelastic surfactant formulations, *J. Non-Newtonian Fluid. Mech.*, 31 (1989) 59.
3. N.S. Berman, Drag reduction by polymers, *Ann. Rev. Fluid Mech.*, 10 (1978) 47.
4. B.A. Toms, Some observations on the flow of linear polymer solutions through straight tubes at large Reynolds numbers, in: *Proceedings of the 1st International Congress of Rheology*, vol. 2, North-Holland, Amsterdam, 1949, Section II, pp.135.
5. N.S. Berman, Drag reduction by polymers, *Ann. Rev. Fluid Mech.,* 10 (1978) 47.
6. J.L. Zakin, D.L. Hunston, Effects of solvent nature on the mechanical degradation of high polymer solutions, *J Appl. Polym. Sci.,* 22 (1978) 1763.
7. C.A. Kim, J.H. Sung, H.J. Choi, C.B. Kim, W. Chun, M.S. Jhon, Drag reduction and mechanical degradation of poly(ethylene oxide) in Seawater, *J Chem Eng. Japan.* 32 (1999) 803.
8. M.D. Warholic, H. Massah, T.J. Hanratty, Influence of drag-reducing polymers on turbulence: effects of Reynolds number, concentration and mixing, *Exp. Fluids.* 27 (1999) 461.
9. M.P. Escudier, F. Presti, S. Smith, Drag reduction in the turbulent pipe flow of polymers, *J. Non-Newtonian Fluid Mech.* 81 (1999) 197.
10. J. Golda, Hydraulic transport of coal in pipes with drag reducing additives, *Chem. Eng. Commun.*, 43, (1986), 53.
11. R.P. Singh, in N.P. Chermisinoff (Ed.), *Encyclopedia of Fluid Mechanics,* Vol. 9, Gulf Publishing, Houston, 1990, Chapter 14.
12. R.A. Mostardi, L.C. Thomas, H.L. Green, F. VanEssen, R.F. Nokes, Suppression of Atherosclerosis in rabbits using drag reducing polymers, *Biorheology.* 15 (1978) 1.
13. A. G. Fabula, Firefighting benefits of polymeric friction reduction, *Trans. ASME J. Basic Eng.*, 93D (1971) 453.
14. H.L. Greene, R.F. Mostardi, R.F. Wokes, Effect of drag reducing polymers on

initiation of Arteriosclerosis, *Polym. Eng. Sci.*, 20 (1980) 499.

15. P.S. Virk, Drag reduction fundamentals, *AIChE J.* 21 (1975) 625.
16. B. Hlavacek, L.A. Rollin, H.P. Schreiber, Drag reduction effectiveness of macromolecules, *Polymer*, 17 (1976) 81.
17. J.L. Lumley, Drag reduction by additives, *Ann. Rev. Fluid Mech.*, 1 (1969) 367.
18. J.L. Lumley, Drag reduction in turbulent flow by polymer additives, *J Polym. Sci. Macromolec.* Rev., 7 (1973) 263.
19. J.L. Lumley, Drag reduction in two phases and polymer flow, *Phys. Fluids.*, 20 (10) (1997) Pt II S64-S71
20. G. Ryskin, Turbulent drag reduction by polymers: A quantitative theory, *Phys. Rev. Lett.* 59 (18) (1987) 2059.
21. P.G. De Gennes, Towards a scaling theory of drag reduction, *Physica.* 140A (1986) 9.
22. P.G. De Gennes, in A. Luigi (Ed), *Introduction to polymer dynamics: An elastic theory of drag reduction*, Cambridge University Press, Cambridge, Great Britain,1990, Chapter 4.
23. H. J. Choi and M. S. Jhon, Polymer-induce turbulent drag reduction, *Ind. Eng. Chem. Res.*, 35 (1996) 2993.
24. J.L. Zakin, B. Lu, H.W. Bewersdorff, Surfactant drag reduction, *Rev. Chem. Eng.*, 14 (1998) 253.
25. G.D. Rose and K.L. Foster, Drag reduction and rheological properties of cationic surfactant formulations, J. Non-Newtonian Fluid Mech., 31 (1989) 59.
26. L.C. Chou, *Ph.D. Dissertation*, The Ohio State University, Columbus, OH, 1991.
27. B. Lu, *Ph.D. Dissertation*, The Ohio State University, Columbus, OH, 1997.
28. T. Nakken, M. Tande, A. Elgsaetr, Measurements of polymer induced drag reduction and polymer scission in Taylor flow using standard double-gap sample holders with axial symmetry, *J. Non-Newtonian Fluid Mech.*, 97 (2001) 1.
29. T. Nakken, M. Tande, B. Nystrom, Effects of molar mass, concentration and thermodynamic conditions on polymer-induced flow drag reduction, *Eur. Polym. J.*, 40 (2004) 181.
30. M. Stickler and N. Sutterlin, in J. Brandrup and E.H. Immergut (Eds.), *Polymer*

Handbook, Concentration dependence of the viscosity of dilute polymer solutions: Huggins and Schulz-Blaschke coefficients, 3rd edition, Vol. 2, A Wiley-Interscience Publication, New York, Chapter 7.

31. W. Brown, J. Fundin, M.D. Miguel, Poly(ethylene oxide)-sodium dodecyl sulfate studied using static and dynamic light scattering, *Macromolecules*, 26 (26) (1992) 7192.
32. B.H. Zimm, Dynamic of polymer molecules in dilute solution: viscoelasticity, flow birefringence and dielectric loss, *J Chem. Phys.*, 24 (1956) 269.
33. K.Y. Mya, A.M. Jameison, A. Sirivat A, Effect of temperature and molecular weight on binding between poly(ethylene oxide) and cationic surfactant in aqueous solutions, *Langmuir*. 16 (2000) 6131.
34. K. Devanand, J.C. Selser, A symptotic behavior and long-range interactions in aqueous solutions of poly (ethylene oxide), *Macromolecules*. 24 (1991) 5943
35. K.Y. Mya, A. Sirivat, A.M. Jamieson, Effect of ionic strength on the structure of polymer-surfactant complexes, *J. Phys. Chem. B.*, 107 (2003) 5460.
36. J. Walowit, S. Tsao, R.C. DiPrima, Stability of flow between arbitrarily spaced concentric cylindrical surfaces including the effect of a radial temperature gradient, *J. Appl. Mech.*, 31 (1964) 585.
37. D. Coles, Transition in circular Couette flow, *J. Fluid Mech.* 21 (1965) 385.
38. E.L. Koschmieder, Turbulent Taylor vortex flow, *J. Fluid Mech.* 93 (1979) 515.
39. P.R. Fenstermacher, H.L. Swinney, J.P. Gollub, Dynamic instabilities and the transition to chaotic Taylor vortex flow, *J. Fluid Mech.*, 94 (1979) 103.
40. J.P. Gollub and H.L. Swinney, Onset of turbulence in a rotating fluid, *Phys. Rev. Lett.* 35 (1975) 927 - 930
41. A.Bouabdallah and G. Cognet, "*Laminat-turbulent transition in Taylor-Couette flow*", in Laminar-Turbulent Transition, ed. By R. Eppler and H. Fasel (Springer, Berlin, Heidelberg, New York 1980) pp. 368 - 377
42. K.Koeltzsch, Y.Qi, R.S. Brodkey and J.L.Zakin, Drag reduction using surfactants in a rotating cylinder geometry, *Exp. in Fluids*, 34 (2003) 515 - 530

43. S. Suksamranchit, A. Anuvat, A.M. Jamieson, Influence of Complex Formation between Poly(ethylene oxide) and Cationic Surfactant on Turbulent Drag Reduction in Aqueous Solution, *J. Colloid and Interface Science,* 294 (2006) 212.

44. B. Lu, X. Li, J.L. Zakin, Y. Talmon, A non-viscoelastic drag reducing cationic surfactant system, J. Non-Newtonian Fluid. Mech., 71 (1997a) 59.

45. B. Lu, Y. Zheng, H.T. Davis, L.E. Scriven, Y. Talmon, J.L. Zakin, Effect of variations in counterion to surfactant ratio on rheology and microstructures of drag reducing cationic surfactant systems, *Rheol Acta*, 37 (1998) 528.

46. Z. Lin, Y. Zheng, H.T. Davis, l.E. Scriven, Y. Talmon, J.L. Zakin, Unusual effects of counterion to surfactant concentration ratio on viscoelasticity of a cationic surfactant drag reducer, *J. Non-Newtonian Fluid Mech.* 93 (2000) 363.

47. B. Lu, F. Li, Y. Kawaguchi, Numerical and experimental investigation of turbulent characteristics in a drag-reducing flow with surfactant additives, *Article in press in Int. Heat and Fluid Flow*, xxx (2004) xxx.

Table 6.1 Various parameters obtained from viscosity and light scattering measurements at different molecular weights of PEO in aqueous solutions at 30°C

Code of system studied	$M_w \times 10^{-5}$ (g/mol)	$[\eta]$ (l/g)	$^{\#}c^*_{PEO}[\eta]$	$D_o \times 10^{12}$ (m^2/sec)	R_h (nm)	$\frac{\mu_2}{\bar{\Gamma}^2}$
PEO1	0.91 ± 0.05	0.100	-	13.3 ± 1.1	16.69 ± 1.4	0.50 ± 0.03
PEO3	3.04 ± 0.34	0.245	0.0123	7.0 ± 0.8	31.71 ± 3.6	0.49 ± 0.03
PEO6	6.06 ± 0.08	0.412	0.0165	5.7 ± 0.3	38.87 ± 2.2	0.39 ± 0.05
PEO9	8.03 ± 0.61	0.503	0.0151	4.6 ± 0.4	48.56 ± 4.2	0.37 ± 0.05
PEO20	17.90 ± 0.37	0.950	0.0143	3.2 ± 0.4	70.24 ± 9.3	0.32 ± 0.05

Note: $^{\#}c^*_{PEO}$ is an optimum PEO concentration for minimum friction factor in pure PEO solutions; $c^*_{PEO3} = 0.05$ g/l, $c^*_{PEO6} = 0.04$ g/l, $c^*_{PEO9} = 0.03$ g/l, $c^*_{PEO20} = 0.015$ g/l.

Table 6.2 Various parameters obtained from light scattering measurement for HTAC, PEO-HTAC and PEO-HTAC-NaCl complex solutions at 30°C

Codes of system studied	PEO M_w (g/mol)	c^*_{PEO} (ppm)	c^*_{PEO} (mM of PEO repeating unit)	$D_o \times 10^{12}$ (m^2/s)	R_h (nm)	$\frac{\mu_2}{\overline{\Gamma}^2}$
#HTAC 1.3 mM	-	-	-	170±2.00	1.31±0.015	0.16±0.01
# HTAC 0.7 mM+[NaCl]/[HTAC] = 1/1	-	-	-	99.8±2.04	2.23±0.045	0.17±0.01
# HTAC 0.6 mM+[NaCl]/[HTAC] = 5/1	-	-	-	90.7±1.53	2.45±0.041	0.07±0.01
PEO6_40+HTAC 5.0 mM	6.06×10^5	40	0.91	3.98±0.20	55.9±2.81	0.83±0.04
PEO6_40+HTAC 5.0 mM+[NaCl]/[HTAC] = 1/1	6.06×10^5	40	0.91	4.92±0.03	45.1±0.23	0.21±0.01
PEO6_40+HTAC 5.0 mM+[NaCl]/[HTAC] = 5/1	6.06×10^5	40	0.91	4.59±0.03	48.4±0.34	0.23±0.01
PEO20_15+HTAC 5.0 mM	17.9×10^5	15	0.34	2.40±0.17	92.7±6.73	0.61±0.03
PEO20_15+HTAC 5.0 mM+[NaCl]/[HTAC] = 1/1	17.9×10^5	15	0.34	3.08±0.05	72.2±1.21	0.25±0.02
PEO20_15+HTAC 5.0 mM+[NaCl]/[HTAC] = 5/1	17.9×10^5	15	0.34	2.90±0.03	76.4±0.81	0.22±0.01

Note: #Light scattering data were determined at the critical micelle concentration; CMC_{HTAC} = 1.3 mM, $CMC_{[NaCl]/[HTAC] = 1/1}$ = 0.7 mM and $CMC_{[NaCl]/[HTAC] = 5/1}$ = 0.6 mM.

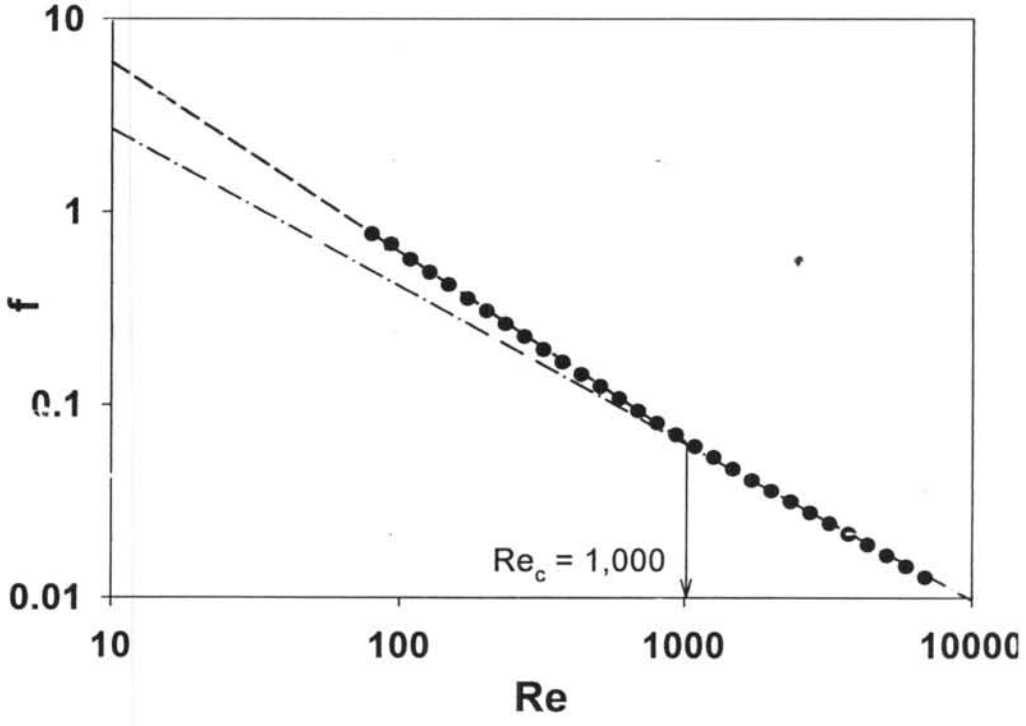

Figure 6.1 Friction factor, f versus Reynolds number, Re of water at 30°C. Re_c is the critical Reynolds number; Re_c of water at 30°C = 1,000.

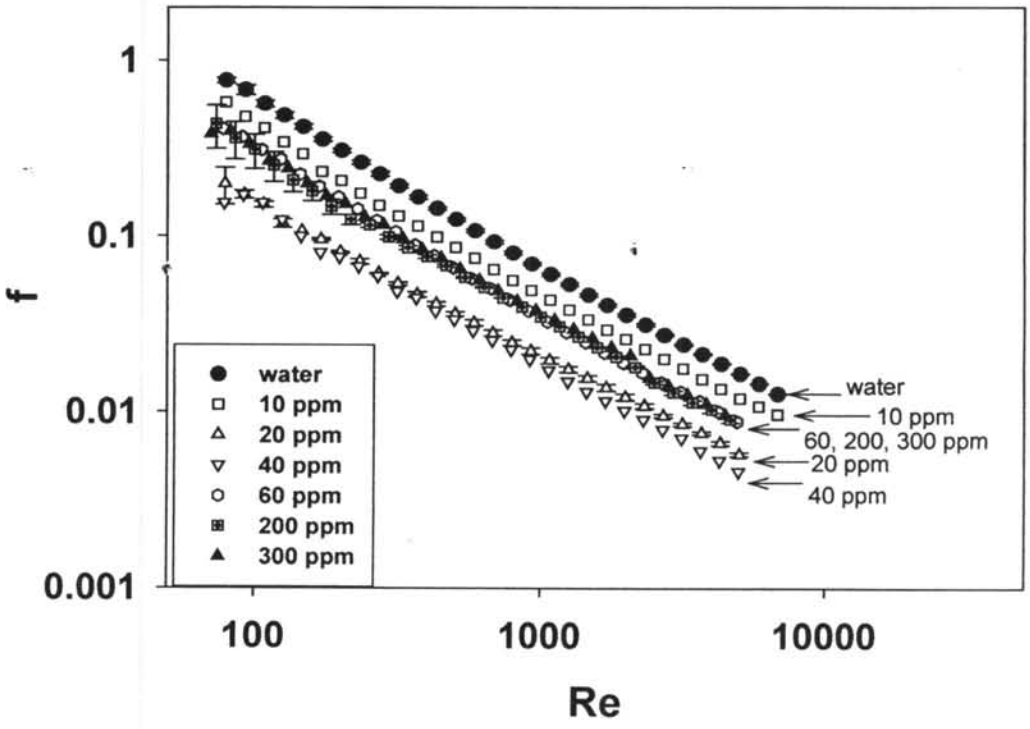

Figure 6.2 Friction factor (f) vs. Reynolds number (Re) at various PEO concentrations of aqueous PEO solutions of PEO6, PEO $M_w = 6.06 \times 10^5$ g/mol, at 30°C.

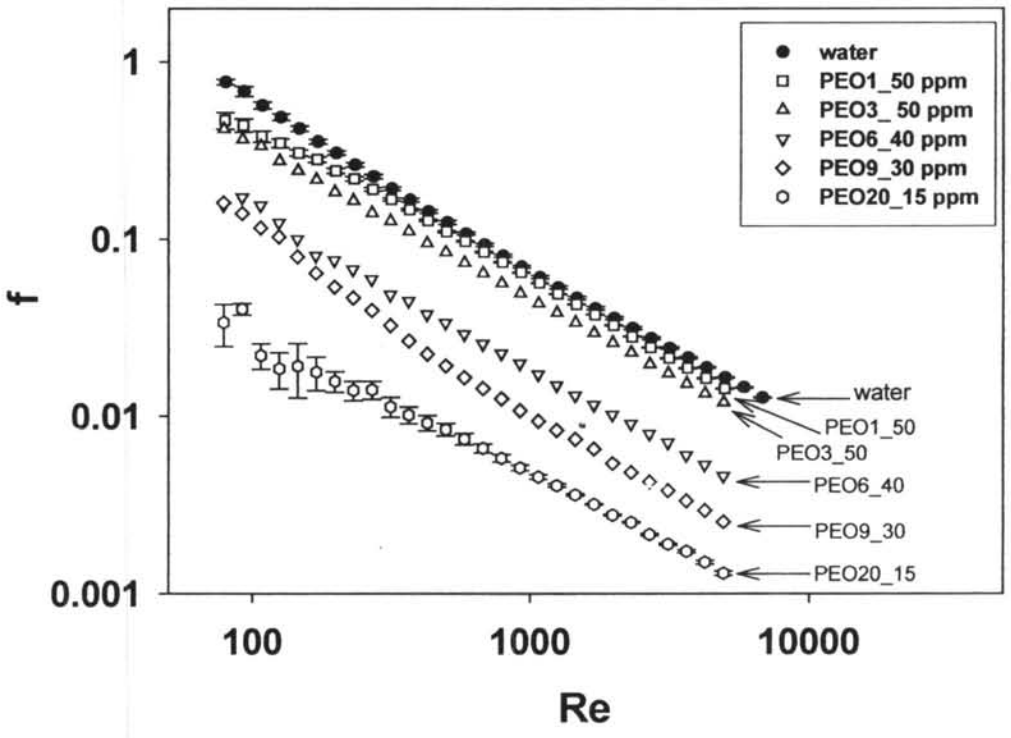

Figure 6.3 Friction factor (f) vs. Reynolds number (Re) at the optimum PEO concentrations of various PEO molecular weights at 30°C: **(a)** PEO1_50 ppm, PEO M_w $0.91x10^5$ g/mol, 50 ppm; **(b)** PEO3_50 ppm, PEO M_w $3.04x10^5$ g/mol, 50 ppm; **(c)** PEO6_40 ppm, PEO M_w $6.06x10^5$ g/mol, 40 ppm; **(d)** PEO9_30 ppm, PEO M_w $8.03x10^5$ g/mol, 30 ppm and **(e)** PEO20_15 ppm, PEO M_w $17.9x10^5$ g/mol, 15 ppm.

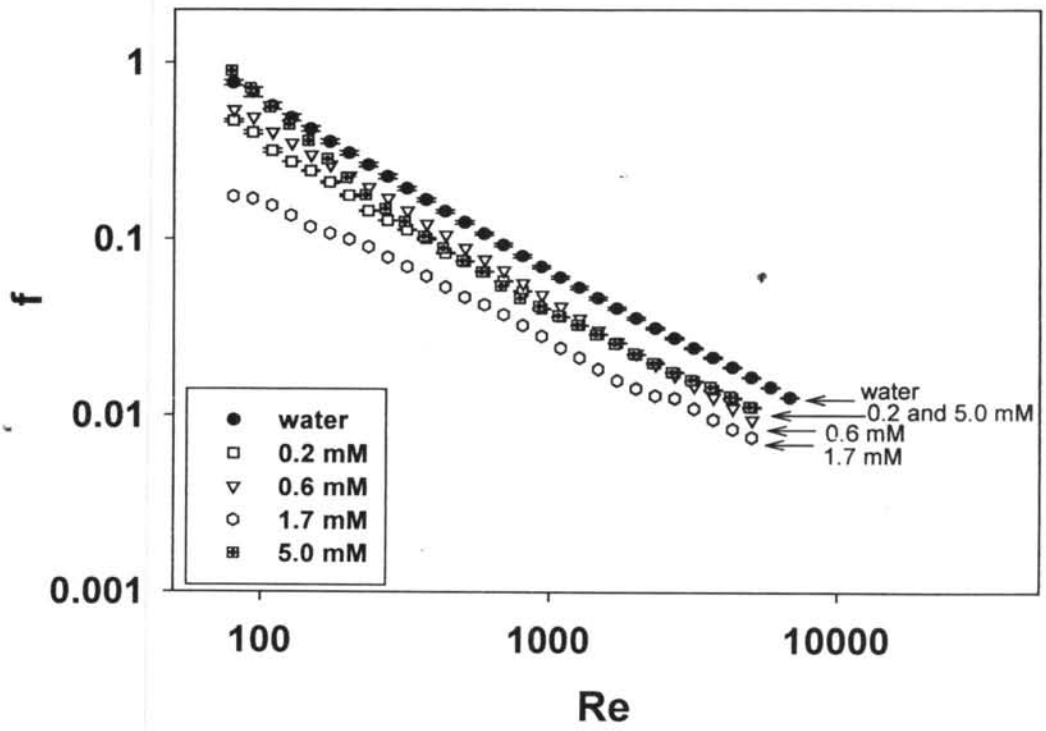

Figure 6.4 Friction factor (f) vs. Reynolds number (Re) at various HTAC concentrations of aqueous HTAC solutions at 30°C. The critical micelle concentration, CMC of HTAC is 1.3 mM.

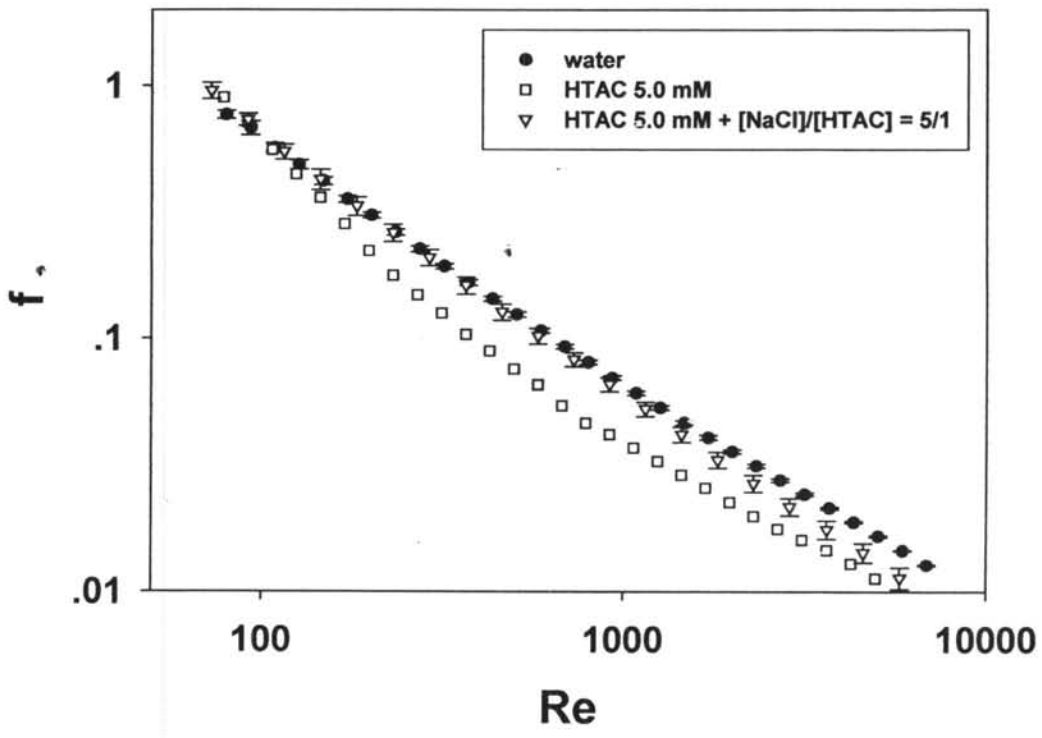

Figure 6.5.1 Friction factor (f) vs. Reynolds number (Re) at 30°C for aqueous solutions of: **(a)** water; **(b)** HTAC 5.0 mM; **(c)** HTAC 5.0 mM + [NaCl]/ [HTAC] = 5/1.

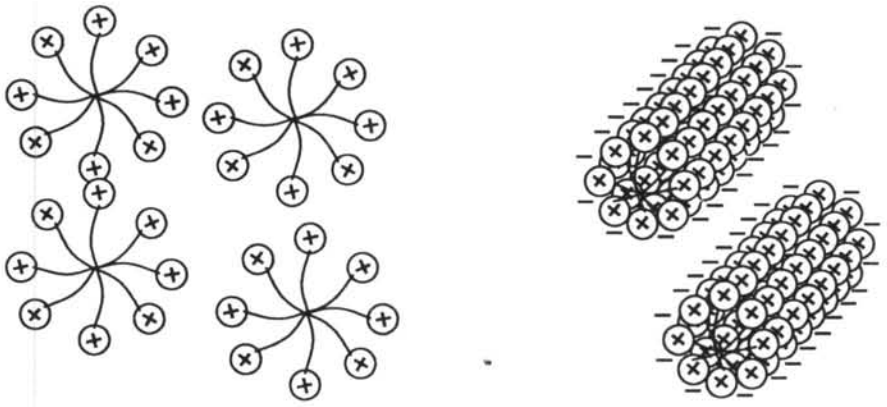

(a) HTAC in aqueous solution *(b) HTAC in NaCl solution*

Figure 6.5.2 Schematic drawings of micelle structures of **(a)** HTAC in aqueous solution and **(b)** HTAC in NaCl solution

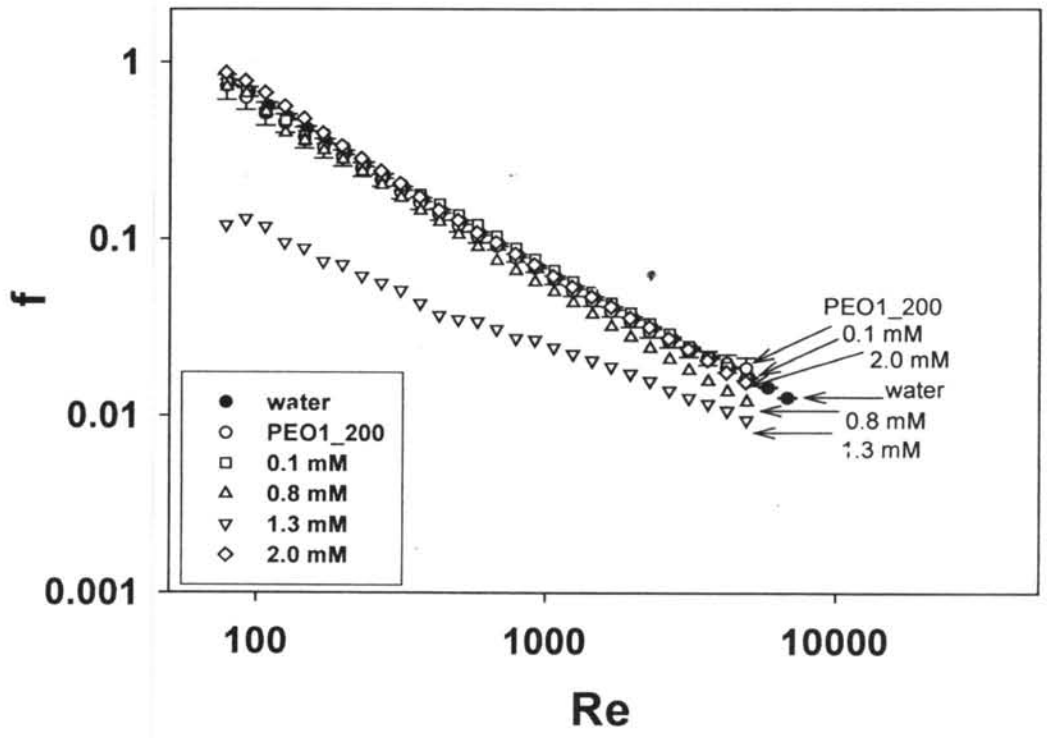

Figure 6.6.1 Friction factor (f) vs. Reynolds number (Re) at various HTAC concentrations and 30°C for aqueous solutions of HTAC/PEO1_200, PEO M_w = $0.91x10^5$ g/mol, 200 ppm. The critical micelle concentration, CMC of HTAC/PEO1_200 is 0.19 mM. The maximum binding concentration, MBC of HTAC/PEO1_200 is 1.80 mM and the critical aggregate concentration, CAC of HTAC/PEO1_200 is 1.90 mM.

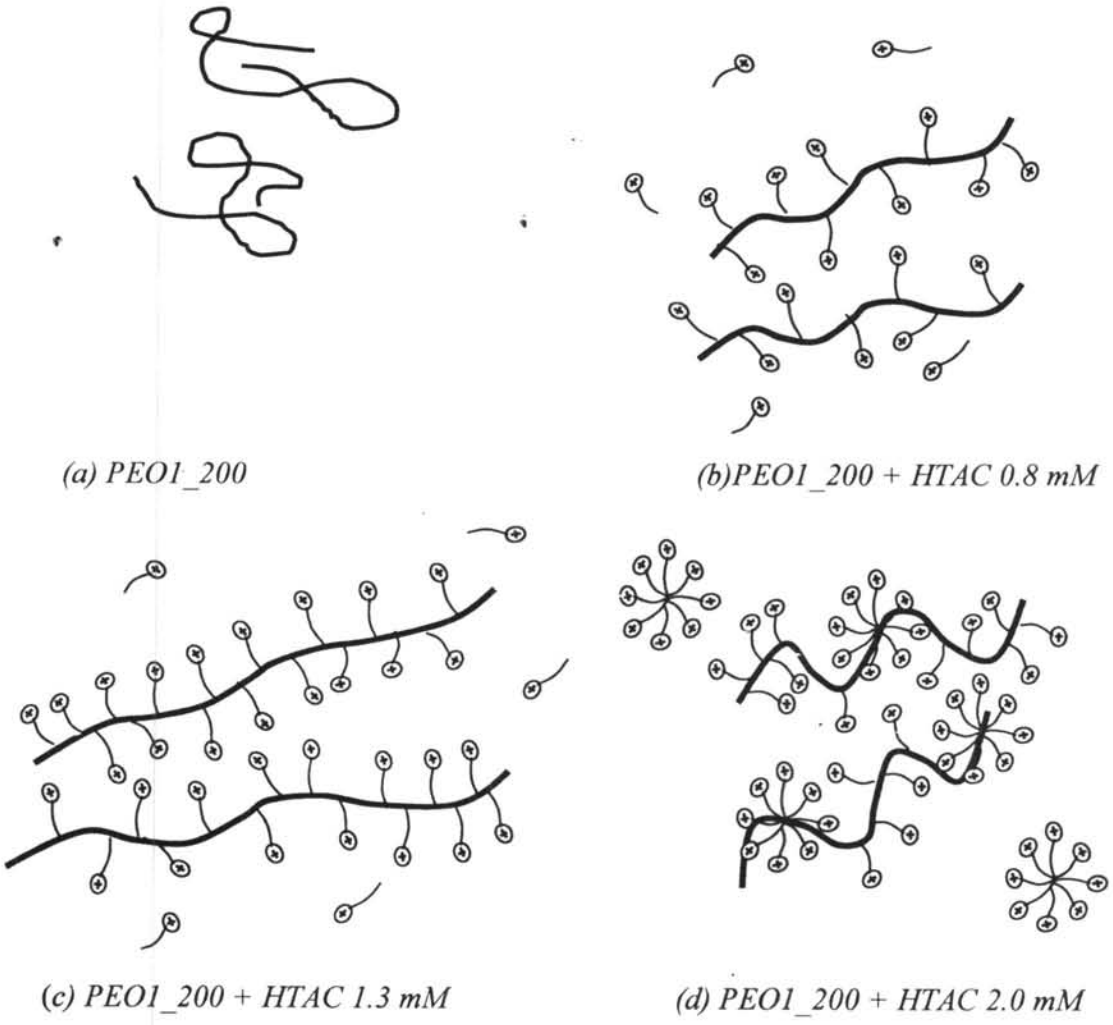

(a) PEO1_200

(b)PEO1_200 + HTAC 0.8 mM

(c) PEO1_200 + HTAC 1.3 mM

(d) PEO1_200 + HTAC 2.0 mM

Figure 6.6.2 Schematic drawings of **(a)** PEO1 at 200 ppm in aqueous solution and **(b) – (d)** the complexes between PEO1 at 200 ppm and HTAC at various HTAC concentrations in aqueous solution.

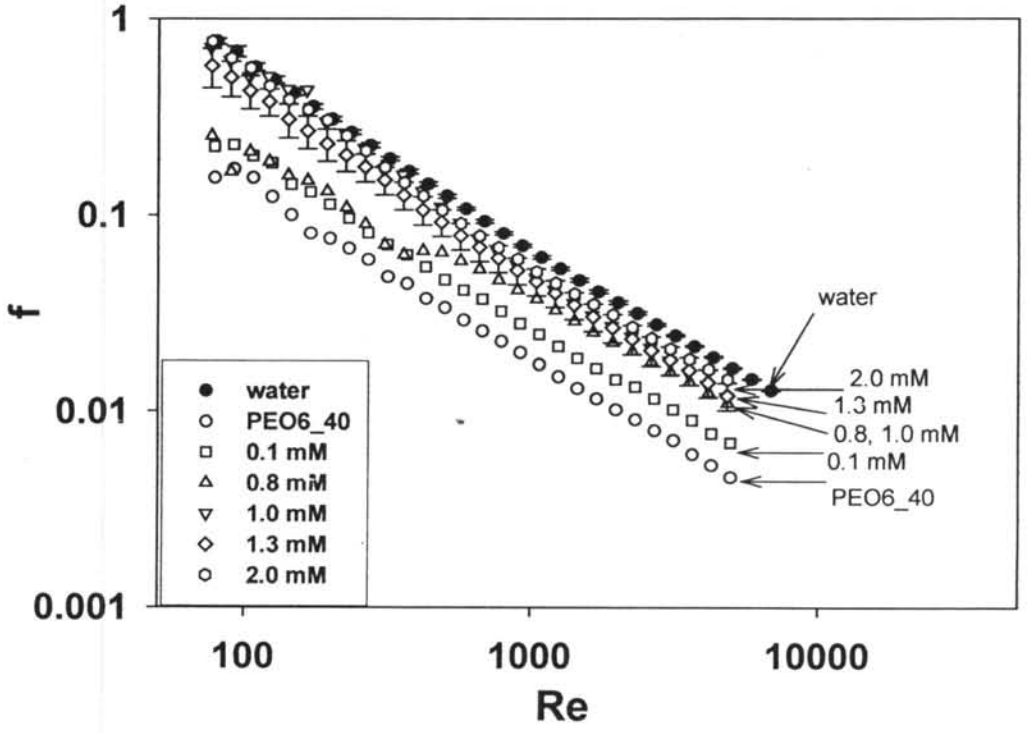

Figure 6.7.1 Friction factor (f) vs. Reynolds number (Re) at various HTAC concentrations and 30°C for aqueous solutions of HTAC/PEO6_40, PEO $M_w = 6.06x10^5$ g/mol, 40 ppm. The critical micelle concentration, CMC of HTAC/PEO6_40 is 0.18 mM. The maximum binding concentration, MBC of HTAC/PEO6_40 is 0.20 mM and the critical aggregate concentration, CAC of HTAC/PEO6_40 is 1.70 mM.

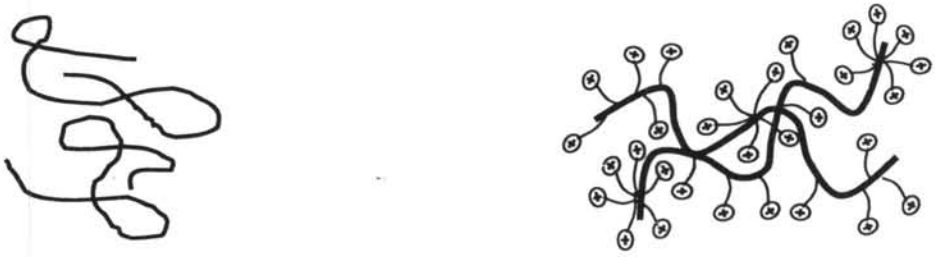

(a)PEO6_40 *(b) PEO6_40 + HTAC*

Figure 6.7.2 Schematic drawings of **(a)** PEO6 at 40 ppm in aqueous solution and **(b)** the complexes between PEO6 at 40 ppm and HTAC in aqueous solution.

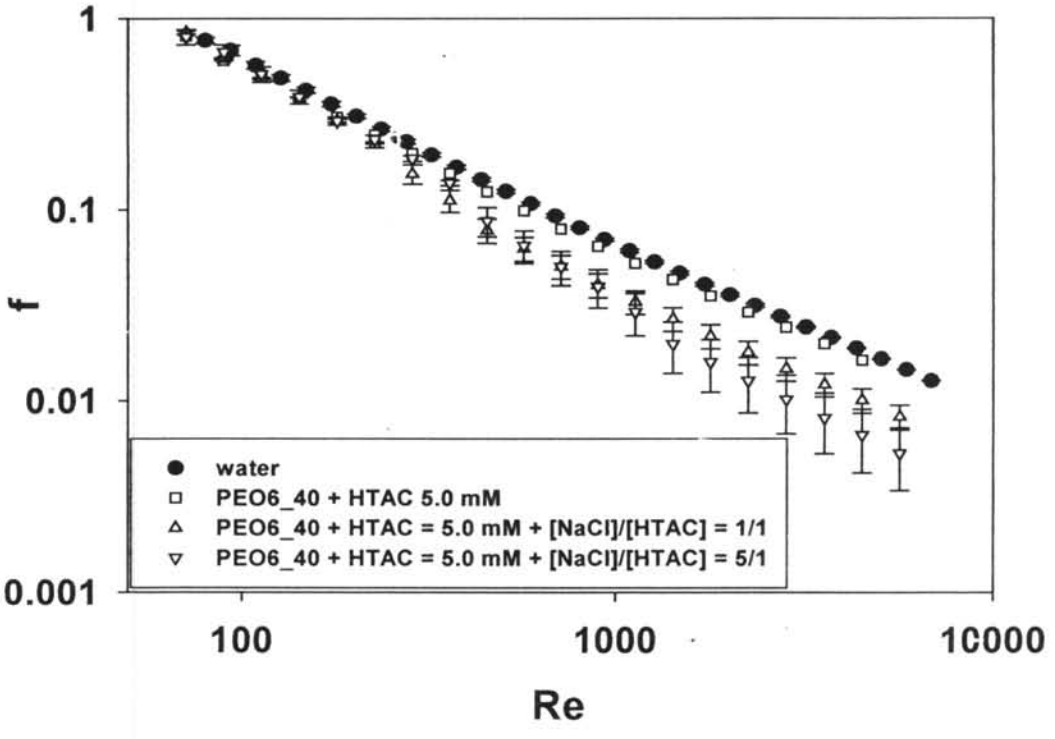

Figure 6.8.1 Friction factor (f) vs. Reynolds number (Re) at 30°C for aqueous solutions of: **(a)** water; **(b)** PEO6_40 + HTAC 5.0 mM, PEO M_w $6.06x10^5$ 40 ppm and HTAC, 5.0 mM; **(c)** PEO6_40 + [NaCl]/[HTAC] = 1/1, PEO M_w $6.06x10^5$, 40 ppm, HTAC 5.0 mM and NaCl, 5.0 mM; **(d)** PEO6_40 + [NaCl]/[HTAC] = 5/1, PEO M_w $6.06x10^5$, 40 ppm, HTAC 5.0 mM and NaCl 25.0 mM.

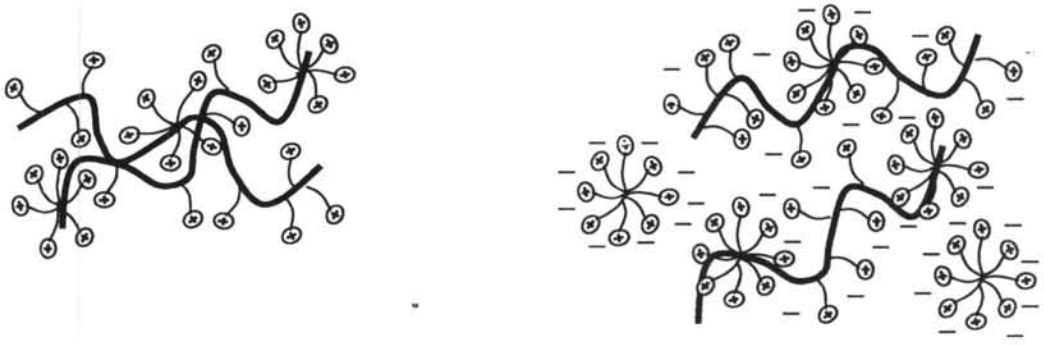

(a)PEO6_40 + HTAC

(b) PEO6_40 + HTAC + NaCl

Figure 6.8.2 Schematic drawings of **(a)** the complexes between PEO6 at 40 ppm and HTAC at 5.0 mM in aqueous solution and **(b)** the complexes between PEO6 at 40 ppm and HTAC at 5.0 mM in NaCl solution.

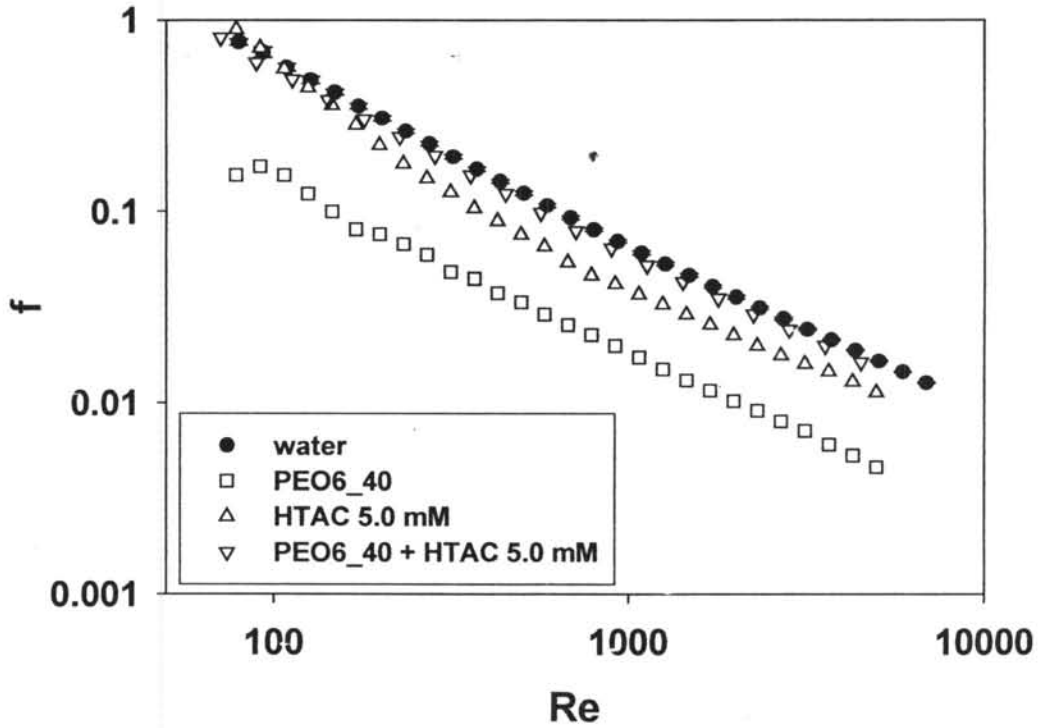

Figure 6.9 Friction factor (f) vs. Reynolds number (Re) at 30°C for aqueous solutions of: **(a)** water; **(b)** PEO6_40, PEO M_w $6.06x10^5$ g/mol, 40 ppm; **(c)** HTAC 5.0 mM; **(d)** PEO6_40 + HTAC 5.0 mM, PEO M_w $6.06x10^5$ g/mol, 40 ppm and HTAC 5.0 mM.